Q. J. R. Meteorol. Soc. (1994), **120**, pp. 1389–1407 551.509.312.21

A pole problem in the reduced Gaussian grid

By P. COURTIER[1]* and M. NAUGHTON[2]
[1] *European Centre for Medium-range Weather Forecasts, UK*
[2] *BMRC, Australia*

(Received 11 June 1993; revised 9 February 1994)

SUMMARY

It is shown that a pole problem may arise from the use of a reduced Gaussian grid in the spectral transform method on the sphere. The problem is related to an asymptotic property of the associated Legendre functions and can be solved by slightly increasing the number of points close to the pole.

It is also shown that the reduced grid controls aliasing arising from quadratic terms only as an asymptotic property. Nevertheless, a small increase in the number of points (everywhere) is enough to reduce the aliasing to a negligible level.

1. INTRODUCTION

Hortal and Simmons (1991) have succeeded in using a reduced Gaussian grid in a shallow-water model and in the primitive-equation model of the European Centre for Medium-range Weather Forecasts (ECMWF). Tests were carried out with Eulerian and semi-Lagrangian advection schemes which demonstrated the ability of the reduced grid to give forecasts that were very similar to those with the full grid, but with a substantial saving in cost.

In the course of the validation which preceded the introduction of the current operational model at ECMWF (T213 spectral truncation), Hortal (1991) and Simmons (1991) noted the presence of noise close to the pole which could be largely removed by using the 'fully reduced grid' instead of the 'fully reduced model' (Hortal and Simmons (1991) terminology). The 'fully reduced grid' and the 'fully reduced model' have the same collocation grid. However, if NLN_k is the number of points at a given latitude row of co-latitude θ_k, and if $NLON$ is the number of points at the equator, then in the fully reduced model $\frac{1}{3}(NLN_k - 1)$ Fourier wave numbers are kept, whereas $\min\{\frac{1}{3}(NLON - 1), (\frac{1}{2}NLN_k - 1)\}$ are kept in the fully reduced grid version. This, however, is not enough, and the number of points of the three latitude rows closest to the pole have been increased from 6, 12 and 18 to 12, 16 and 20. Furthermore, in the Eulerian version of the model the noise accompanied the (u, v) formulation of the model and not the vorticity–divergence formulation.

Figure 1 shows the 300 hPa vorticity field of the noisy 72-hour forecast referred to by Simmons (1991) and Hortal (1991) using the fully reduced model. At both the northern and southern poles, the field is noisy. The difference with the noise-free forecast obtained using the fully reduced grid and with an increased number of points close to the pole is depicted in Fig. 2.

Hortal and Simmons (1991) determined the number of points N_k of a given latitude row of co-latitude θ_k by requiring the distance between two adjacent points on this row of latitude to be the largest possible, fulfilling the constraints imposed by the fast Fourier transform (FFT), but smaller than the distance apart of two adjacent points at the equator. We have thus $NLN_k \geqslant NLON \sin\theta_k$. In the following we shall call the grid

* Corresponding author: European Centre for Medium-range Weather Forecasts, Shinfield Park, Reading, Berkshire RG2 9AX, UK.

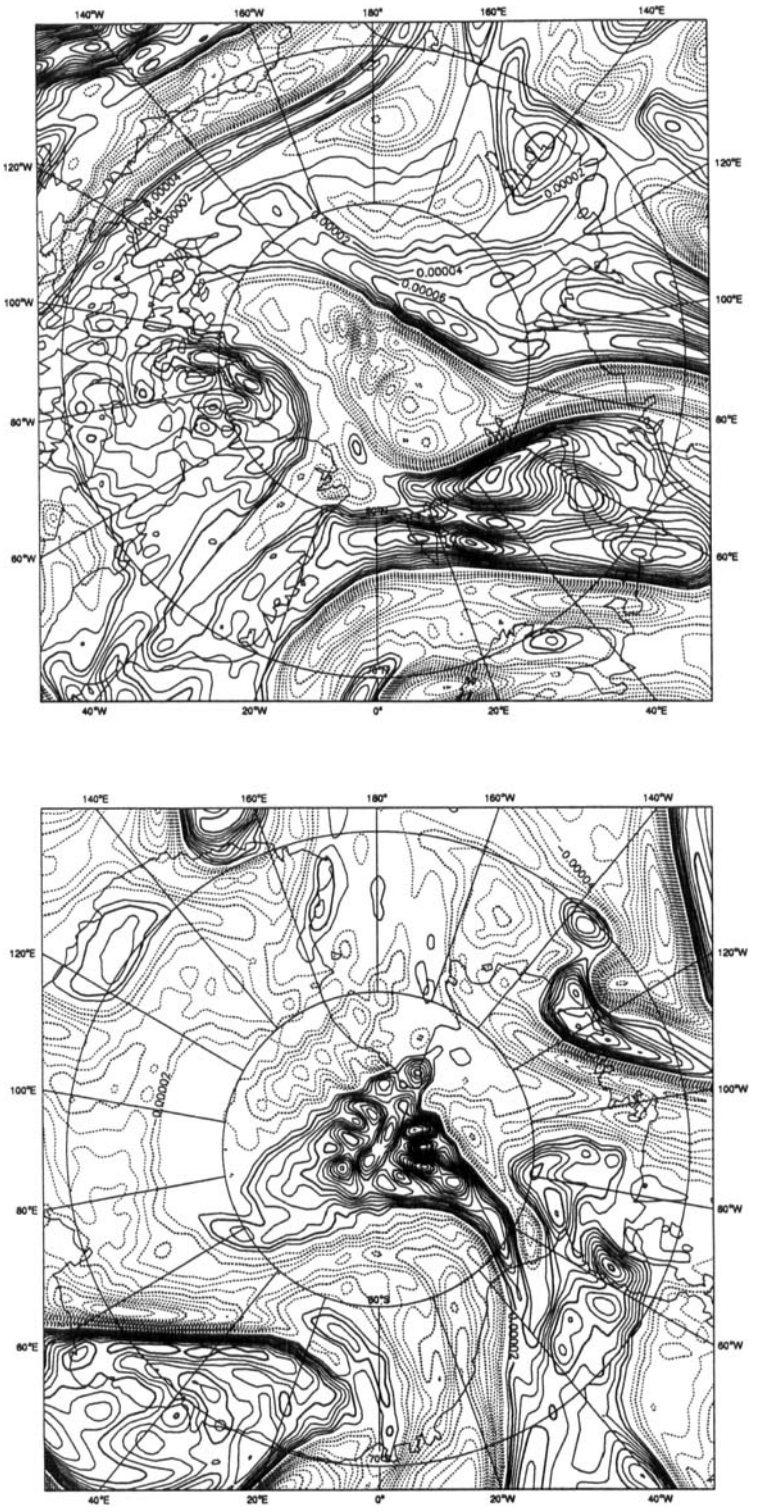

Figure 1. 300 hPa vorticity field of a 72-hour forecast obtained using the fully reduced model (T213 L31, semi-Lagrangian). Initial date: 15 January 1991, 12 UTC. Top: northern pole area. Bottom: southern pole area; isoline: $1 \times 10^{-5} s^{-1}$. (Courtesy of Adrian Simmons.)

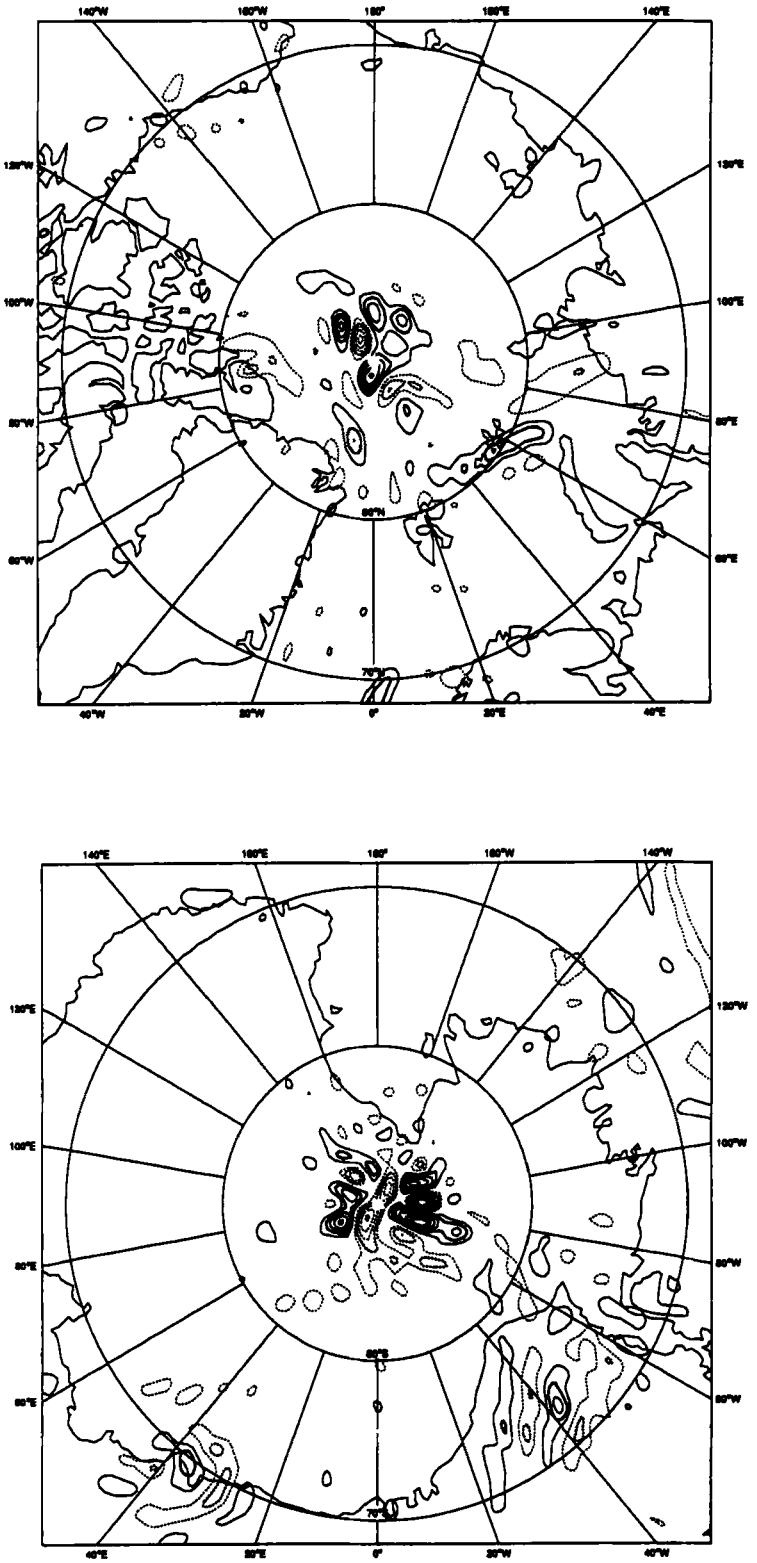

Figure 2. Same as Fig. 1 but for the difference: fully reduced model − fully reduced grid; isoline: $1 \times 10^{-5} s^{-1}$.

which has $NLON \sin \theta_k$ points the 'geometric reduced grid'. Note that the term 'geometric-reduced grid' is only a theoretical concept and, in particular, that it has a non-integer number of points. On a given latitude row Hortal and Simmons (1991) then used a number of points which was the first number larger than the geometric-reduced grid and which fulfilled the constraints arising from the FFTs.

Jarraud and Simmons (1983) simulated the effect of a reduced grid by resetting to zero those values of the associated Legendre function which were below a given threshold, ε. They did this in a model using a full grid, but this is equivalent to neglecting, in the Gaussian quadrature, the wavenumber m greater than a certain value depending on the latitude row. This did not exactly mimic a reduced grid in that no aliasing errors may be introduced in the east–west direction in the Fourier transforms, nevertheless it was considered successful as a feasibility study.

These two approaches rely on different intuitive ideas: in the first, one seeks a quasi-homogeneous grid (the argument is geometric), whereas in the second, one neglects small contributions (it relies on spherical harmonic properties). We shall refer to the ε-reduced grid as that reduced grid which is obtained using the following procedure. For a given row of latitude, we first identify the associated Legendre functions whose absolute value is greater than ε, and consider $m_{\max}$ the maximum value of m thus obtained. The number of points of the ε-reduced grid is then, in the case of the linear grid, the lesser of $(2m_{\max} + 1)$ and the number of points of the full grid, and in the case of the alias-free grid is the lesser of $(3m_{\max} + 1)$ and the number of points of the full grid (Bourke 1972).

The purpose of this paper is first to suggest a possible reason why Hortal (1991) and Simmons (1991) had to use more points close to the pole, highlighting a weakness of the geometric-reduced grid close to the pole, and secondly to establish the convergence of the ε-reduced grid to the geometric-reduced grid at a given latitude and for large total wavenumbers, n.

2. The problem close to the pole

In Fig. 3 is shown the maximum, over a total wavenumber n, of the orthogonality error of the associated Legendre functions of given zonal wavenumber m where the Gaussian quadrature is performed neglecting those latitude rows closer to the pole than a given latitude row (ordinate). This orthogonality is computed within a T106 truncation and for a Gaussian quadrature of 80 points in a hemisphere, which is the number usually used for a T106 model. The scale is logarithmic which means that the -4 isoline corresponds to an error of 10^{-4}.

We are thus introducing another concept which we shall call an ε'-reduced grid. If we introduce the term $m_s(\theta_k)$ as the smallest wavenumber that is discarded for a given latitude row of co-latitude θ_k, and the term $\theta_s(m)$ as the co-latitude of the closest latitude row from the equator which is discarded for a given zonal wavenumber (because the associated Legendre functions $P_n^m(\cos\theta)$ decrease towards zero approaching the pole there is clearly a one-to-one relationship between $m_s(\theta_k)$ and $\theta_s(m)$), then the ε-reduced grid and the ε'-reduced grid differ in the choice of criteria. In the ε-reduced grid the reliance is on the value of the Legendre polynomial, whereas in the ε'-reduced grid it is on their orthogonality.

For a given wavenumber m we have

ε-reduced grid:

$$\max_n |P_n^m(\cos\theta_k)| \leq \varepsilon \qquad \text{for all } \theta_k \leq \theta_s \tag{1}$$

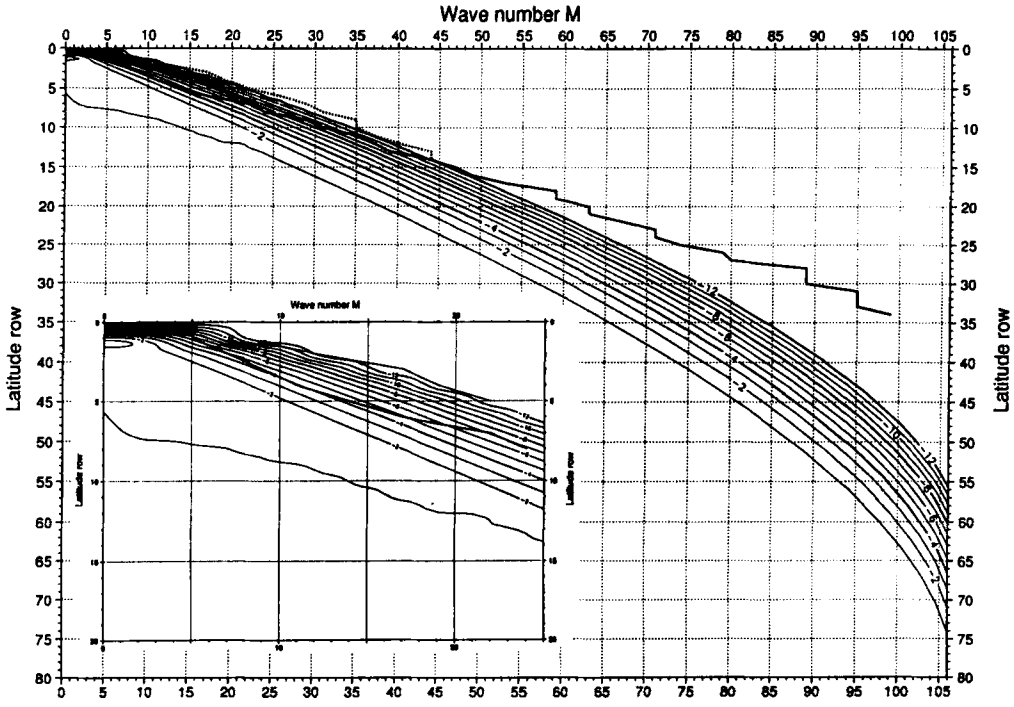

Figure 3. Logarithm of the error of the orthogonality within a T106 truncation of the associated Legendre functions of a given zonal wavenumber m (abscissa) and of the total wavenumber varying from m to 106 when the Gaussian quadrature is performed neglecting the latitude rows closer to the pole than a given latitude row (ordinate). The bottom left insert is an enlargement of the pole area. See text for the solid and dashed curve.

ε'-reduced grid:

$$\max_{n,n'} \left| \sum_{\theta_k \leq \theta_s} P_n^m(\cos\theta_k) P_{n'}^m(\cos\theta_k) w(\theta_k) \right| \leq \varepsilon' \tag{2}$$

where $w(\theta_k)$ denotes the Gaussian weight.

The spectral technique is a Galerkin method (Dautray and Lions 1985) in which the basic functions are orthogonal. It is possible to implement a Galerkin method with non-orthogonal basic functions (like finite elements) but then it is essential to account for the mass matrix which consists of the scalar product of the basic functions. This is the reason for using the ε'-reduced grid for practical purposes, since the mass matrix differs from the unit matrix by values of, at most, ε'. There is some arbitrariness concerning the maximum of the orthogonality error (which is associated with an L^∞ norm) and one might have considered an L^2 norm where the sum of the square of the error is considered instead of the maximum. However, we preferred the L^∞ norm since it is more sensitive to outliers than the L^2 norm. Furthermore, in grid-point space the pole problem is concentrated in a localized geographical area, as it is to some extent in spectral space, as we shall see later. In Appendix 1, we show that ε' should vary as n^{-1} so as to keep the error introduced in the Galerkin formulation below a given threshold.

A theoretical analysis of the ε'-reduced grid is, however, difficult since it involves integrals computed using discrete sums, whereas the ε-reduced grid involves only associated Legendre function values. A notable and easy particular case is when only the first

latitude row is discarded in the ε'-reduced grid. Results of convergence or non-convergence of the ε-reduced grid do not imply that they are valid for the ε'-reduced grid. Nevertheless, we shall see that, in the range 21 to 213, the behaviour of the ε'-reduced grid is similar in practice to the theoretical results obtained for the ε-reduced grid.

The thick line of Fig. 3 corresponds to the number of points NLN_k proposed by Hortal and Simmons (1991) with the previously mentioned increase close to the pole. One immediately notices that there is a problem close to the pole (from latitude row 1 to 13). The maximum error reaches 10^{-4}, which is confirmed by looking at the error obtained for meteorological fields, going from spectral space to the reduced grid and then back again to spectral space (as we shall discuss in the conclusion). The change made by Hortal (1991) and Simmons (1991), namely, going from 6, 12, 18 to 12, 16, 20 at rows 1, 2 and 3, had the effect of going from an error of 10^{-2} to one of 10^{-4}.

It is easy to generate the grid which will preserve an orthogonality within 10^{-12}, by increasing when necessary the number of points to more than NLN_k, while fulfilling the FFT constraints. This corresponds to the dotted line in Fig. 3. One may notice that, after wavenumber 50, the error is far above the -12 isoline. This arises from the fact that the grid used by Simmons (1991) and Hortal (1991) is constrained by an alias-free property. Bearing this in mind, we therefore do not propose to decrease the number of points after wavenumber 50; the issue here is to increase the grid so as to have the mass matrix differing from unity by less than ε. A threshold of 10^{-12} is chosen since it corresponds to the order of magnitude of the error, when using the full grid, due to the roundoff errors in the computation of the Legendre transforms done on a 64-bit arithmetic machine. In Table 1 we present the number of points obtained which should be compared with the values originally proposed by Simmons (1991) and Hortal (1991).

TABLE 1. NUMBER OF POINTS CLOSE TO THE POLE OF THE REDUCED GRID OF A T106 MODEL

Latitude row	Number of points necessary for an orthogonality of 10^{-12}	Number of points proposed by Hortal (1991) and Simmons (1991)
1	18	12
2	25	16
3	36	20
4	40	24
5	45	30
6	54	36
7	60	45
8	64	50
9	72	60
10	72	64
11	75	72
12	81	75
13	90	80
14	90	90
.	.	.
.	.	.
.	. ← identical →	.

Figures 4 and 5 are the same as Fig. 3 but for a T213 and a T42 truncation, respectively. It is worth noticing that the amplitude of the pole problem is very similar in each case and for almost the same number of rows of latitude (which are obviously at a different geographical latitude): 13 at truncation 42 and 106, 16 at truncation 213.

Such a weak dependency on truncation suggests that the effect may be related to an asymptotic property of the associated Legendre functions close to the pole singularity.

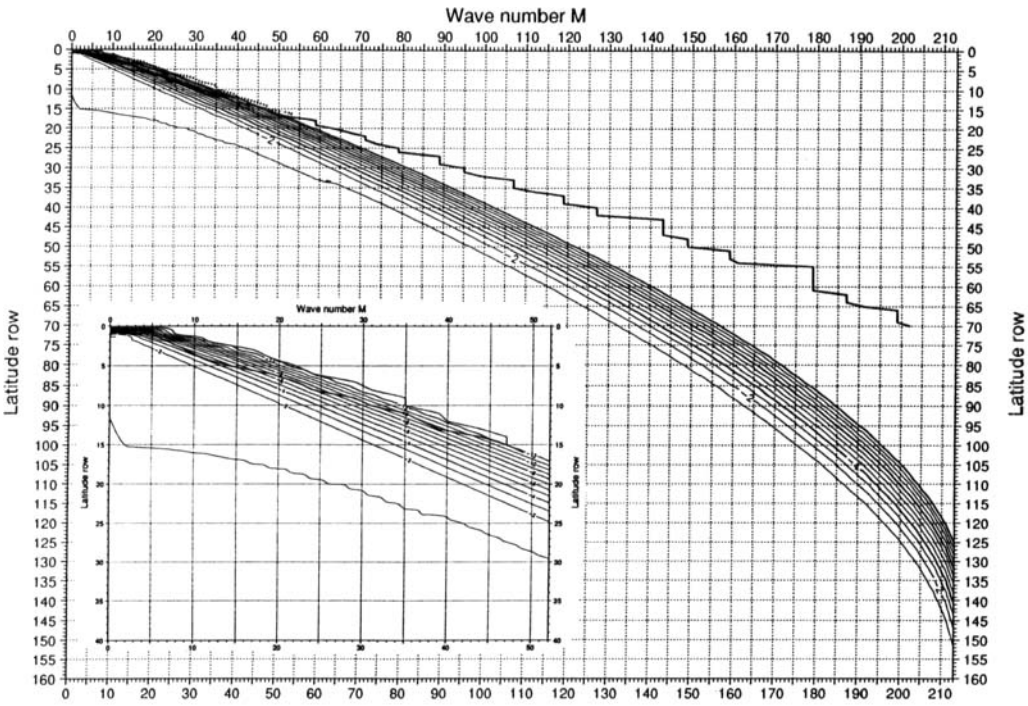

Figure 4. Same as Fig. 2 but for a T213 truncation.

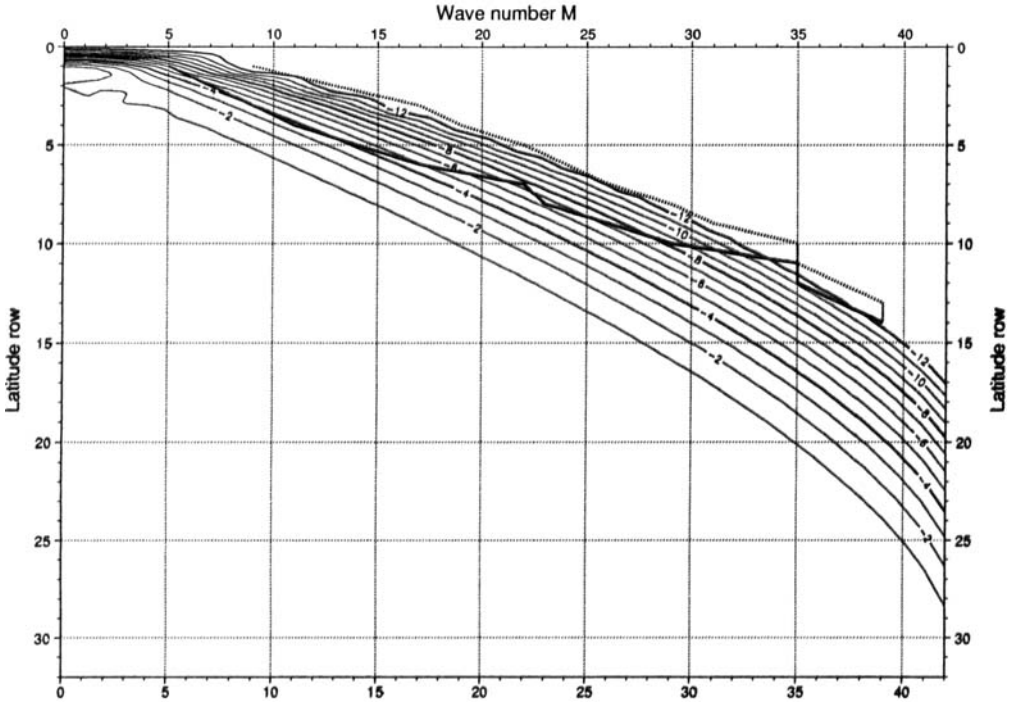

Figure 5. Same as Fig. 1 but for a T42 truncation.

In Appendix 2, the following asymptotic result is demonstrated. For a given k (row of latitude index of the Gaussian grid, $k = 1$ is the closest to the pole) and for a given zonal wavenumber, m,

$$P_n^m(\cos\theta_k) = (2n)^{1/2}\{J_m(x_k) + O(n^{-1})\} \tag{3}$$

where

$$x_k = \frac{4k-1}{6}\pi\left\{1 + \frac{2}{(4k-1)^2\pi^2}\right\},$$

J_m is the Bessel function of the first kind and θ_k is the co-latitude of the k^{th} latitude row of the Gaussian grid. It tends towards the northern pole as n tends toward infinity. (Only the northern pole is considered; the behaviour at the southern pole follows from the symmetry properties of the associated Legendre functions). Here we are considering the Gaussian grid of a T_n model which has a number N of latitude rows large enough to prevent the aliasing errors arising from the quadratic terms (Bourke 1972).

$$n = \text{Int}\left(\frac{2N-1}{3}\right)$$

where 'Int' stands for 'the integer part of'.

For the first latitude row ($k = 1$) of the T_n grid we have

$$P_n^m(\cos\theta_1) \approx (2n)^{1/2}J_m(x_1)$$

with $x_1 \approx 1.6$.

As $J_m(1.6)$ decreases by an order of magnitude as m varies from 8 to 9, and as $(2n)^{1/2}$ increases only slowly (9 at T42, 14.6 at T106 and 20 at T213), the number of points necessary on the first row of latitude remains the same for these three truncations in an ε-grid (with $\varepsilon = 10^{-5}$, say). This is compatible with what is obtained for the ε'-grid, as can be seen in Figs. 3, 4 and 5 where the wavenumber m for the first latitude row has the values 8, 8 and 9, respectively (for truncation 106, 213 and 42), which corresponds to 18, 18 and 20 points. Another interesting feature is that the number of points necessary on the first row of latitude for the ε-grid will increase toward infinity as n tends to infinity. For any given m, there exists some n such that $P_n^m(\cos\theta_1)$ is greater than any given positive real number. However, the increase of m (and thus of the number $2m + 1$ of points necessary to keep $P_n^m(\cos\theta_1)$ below a given threshold, e.g. 10^{-6}, depends on the variation of $J_m(\theta_1)$ as a function of m. In the vicinity of $m = 8$, J_m decreases by one order of magnitude for each increase of m by 1 unit; as a consequence, m would then increase as $\frac{1}{2}\log_{10} n$. In contrast, the number of points of the geometric reduced grid is asymptotically constant and equal to $2x_k$ (3.2 at the first latitude row).

We have shown that the number of points necessary on the first row of latitude of the ε-grid was increasing slowly. One should notice that we have established a necessary condition only for the ε-grid: it must have more than the number of points discussed above. That is not a sufficient condition since we have not shown that, for all m larger than, say 8, the associated Legendre functions are smaller than ε.

Let us apply the asymptotic result to the first latitude row of the ε'-reduced grid. Combining (2) and (3) we get the maximum orthogonality error for $n = n'$ which behaves as $n\{J_m(x_1)\}^2 w(\theta_1)$. The Gaussian weights, $w(\theta_k)$, are given by

$$w(\theta_k) = \frac{2N+1}{\sin^2\theta_k\, P_N'^0(\cos\theta_k)^2}$$

where $N = 1.5n$ for a Gaussian grid. Differentiating formula (A.2.2) from Appendix 2

and combining with the above expression for $w(\theta_k)$, we find, for small values of k, that

$$w(\theta_k) \approx \frac{1}{\{1.5n J_0'(x_k)\}^2}.$$

The maximum orthogonality error then becomes

$$\frac{1}{n}\left\{\frac{J_m(x_1)}{1.5J_0'(x_1)}\right\}^2$$

and decreases as n^{-1}. As a consequence of the decrease of the error, the number of points of the ε'-reduced grid decreases slowly. If we change the criteria with n, as suggested in Appendix 1, the decrease as n^{-1} is what is necessary to keep below a threshold the errors introduced by the assumption that the mass matrix is equal to its inverse. The number of points of this grid then becomes constant asymptotically.

In the graph presented for the ε'-reduced grid, one does not see a variation in n^{-1} since it is hidden by the large variation of $J_m(1.6)$ with m (one order of magnitude for a change in m of 1). It is worth noticing that the value $m = 8$, numerically found at truncation 106, is compatible with the above asymptotic formula, since, for $m = 7$, the formula predicts an error of 1.9×10^{-11}, and for $m = 8$ it predicts 1.9×10^{-13}. The chosen threshold 10^{-12} is in between.

3. THE SIMPLE CONVERGENCE OF THE ε-REDUCED GRID TO THE GEOMETRIC-REDUCED GRID

In this section we show that, for a given co-latitude θ, the number of points of the ε-reduced grid converges toward the number of points of the geometric-reduced grid. This result is suggested by the behaviour shown in Figs. 3, 4, 5: at T42, T106, T213 the latitude rows 4, 10, 25 are at approximately the same co-latitude, θ, and the 10^{-12} isoline is crossed at $m = 18.5$, 34, 39, respectively, which increase more slowly than the truncation. The corresponding maximum values of m for the geometric grid are $m = 12$, 31, 62, so it is clear that additional resolution is required by the ε'-reduced grid at T42 and marginally still at T106, but not at T213.

The number of points of the geometric-reduced grid is $NLON \sin\theta$. Let us denote by NL_ε the number of points of the ε-reduced grid. By convergence of the ε-reduced grid towards the geometric-reduced grid, we mean that

$$\lim_{NLON\to\infty} \frac{NL_\varepsilon}{NLON \sin\theta} = 1.$$

As NL_ε and $NLON \sin\theta$ are related to the maximum wavenumber retained by the same proportionality factor, the convergence property may be expressed in terms of maximum wavenumber considered for a given co-latitude θ: M_ε for the ε-reduced grid and $M \sin\theta$ for the geometric grid (M being the value at the equator). Furthermore, $NLON$ is proportional to the truncation n if we consider a Gaussian grid (either linear or alias-free for the quadratic terms). The convergence criterion becomes

$$\lim_{n\to\infty} \frac{M_\varepsilon}{M \sin\theta} = 1.$$

If we define ϕ_ε by $M_\varepsilon = M \sin\phi_\varepsilon$, we then have to show that

$$\lim_{n\to\infty} \phi_\varepsilon = \theta.$$

In Appendix 3 we show that

$$\lim_{\substack{n\to\infty \\ m=n\sin\phi}} P_n^m(\cos\theta) = 0 \qquad \text{for all } \phi > \theta.$$

Furthermore, we show that there is uniform convergence in any interval $[\psi, \pi/2]$ if $\psi > \theta$. This may be expressed in the following way: For all ε greater than zero and all ψ greater than θ there exists some n_0 such that for all n greater than n_0 and all ϕ greater than ψ, $m = n \sin\theta$ and $|P_n^m(\cos\theta)| < \varepsilon$. For a given ε, let us apply this result to the case $\psi = \theta + \varepsilon$. Then there exists some n_0 such that for all n greater than n_0 and all ϕ greater than ψ, $|P_n^m(\cos\theta)| < \varepsilon$. This means that ϕ_ε is necessarily smaller than $\theta + \varepsilon$; the convergence has thus been demonstrated.

4. Non-linear aliasing on the reduced grid

The result of the previous sections can be used to study the properties of a grid which has $3m + 1$ points on each latitude row, so as to avoid aliasing errors due to the quadratic terms in the equations (Bourke 1972). Figure 6 is the same as Fig. 3, but the orthogonality is computed for a T106 truncation with respect to a T212 truncation. The thick curve, as in Fig. 3, corresponds to the grid used by Hortal (1991) and Simmons (1991). The wavenumber associated with *NLN* points in an alias-free Fourier transform is $\frac{1}{3}(NLN\text{-}1)$ which corresponds to the fully reduced grid. One should note that these authors are proposing the fully reduced model in which the number of waves retained is $\min\{\frac{1}{2}(NLN\text{-}1), \frac{1}{3}(NLON\text{-}1)\}$. This means that when $\frac{1}{2}(NLN\text{-}1) < \frac{1}{3}(NLON\text{-}1)$ they are

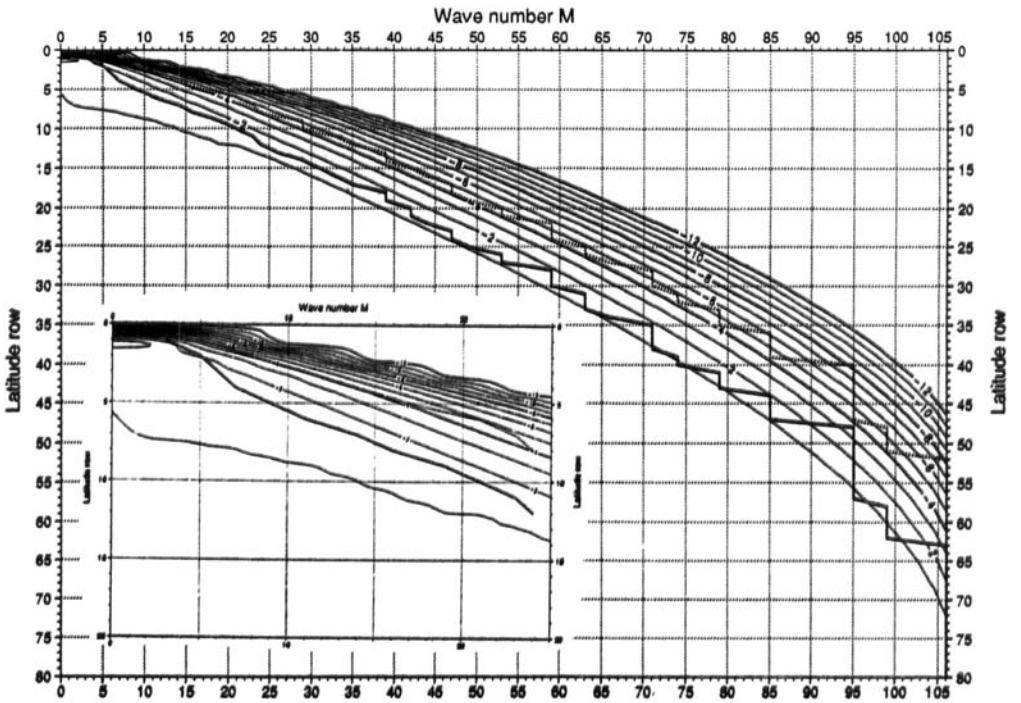

Figure 6. Same as Fig. 1 but for the aliasing errors due to the quadratic terms in a T106 model. The orthogonality is computed for a T106 truncation but with the associated Legendre functions of a T212 truncation.

incurring more aliasing in the E–W direction in the Fourier transform with less aliasing in the N–S direction in the Legendre transform. They have gone from one extreme to the other; intermediate solutions might have been better, but this would have required a bidimensional analysis. The solid line lies between the -1 and the -2 isolines most of the time, which shows that the aliasing errors reach 10^{-1}. The 10^{-4} reduced grid compatible with the FFTs corresponds to the dotted line. The number of points of this grid is 37 576, to be compared with the 33 766 points corresponding to the thick line. This represents an increase of 11%. In Appendix 3, we see that the associated Legendre functions converge toward zero exponentially, which implies that the surface in between the -12 and the -1 isolines is halved when the resolution is doubled (which is what we find in practice). As a consequence, the number of extra points increases linearly with n, which shows that the extra cost at T213 is half of what it is at T106.

Here we proposed 10^{-4} as a threshold; this is based on experimentation performed at Météo-France with an aqua-planet model (El Khatib, personal communication). A 10^{-12} criterion would be a waste of resources since aliasing from cubic or higher-order terms is present anyway. It is likely that a less conservative threshold, such as 10^{-2}, would be a better compromise—cost versus performance.

5. Conclusion

In Fig. 7 is shown the difference between a vorticity field and what is obtained after going 300 times from spectral to grid-point space and back again to spectral space. The number 300 has been selected since it is the number of time-steps associated with the 72-hour forecast mentioned in the introduction. The original vorticity field corresponds to the noise-free field that has been produced by Simmons (1991). The number of points in use close to the pole corresponds to the geometric grid: 6, 12 and 18 on the first three latitude rows. Some noise is clearly noticeable, which is in agreement with the theoretical analysis of section 2. Its magnitude is $2 \times 10^{-6}\text{s}^{-1}$, which corresponds to a few percent of the vorticity field. This, however, is smaller than in Fig. 2 by two orders of magnitude. Amplification by means of the dynamics or aliasing errors is thus a necessary aid to get from Fig. 7 to Fig. 2. In Fig. 8, as in Fig. 7, is shown what is obtained from using 12, 16 and 20 points on the first three latitude rows, as proposed by Simmons (1991) and Hortal (1991). A noise pattern is still present, which moves equatorwards in agreement with the thick line in Fig. 3, where the maximum error is no longer at the first latitude row, but at the fourth. The maximum is $3.5 \times 10^{-8}\text{s}^{-1}$ and is reduced by two orders of magnitude compared to Fig. 7.

We have checked that the problem is cumulative: the noise obtained going 300 times from spectral to grid-point and back again is almost equal to 300 times the noise produced going only once from spectral to grid-point and back. In the course of a model integration, this acts as a permanent noise generator.

The increase in the number of points close to the pole, found necessary by Hortal (1991) and Simmons (1991), is most likely due to the asymptotic property of the associated Legendre functions, the consequence of which is that the ε-reduced grid does not converge uniformly to the geometric-reduced grid. In addition, we have shown that there is convergence (for a given latitude) of the ε-reduced grid to the geometric-reduced grid. Furthermore, the use of the geometric grid leads to aliasing errors of order of magnitude 10^{-1}. The difference in behaviour of the u–v formulation and the vorticity–divergence formulation is thus likely to be related to differences of aliasing of the pressure gradient

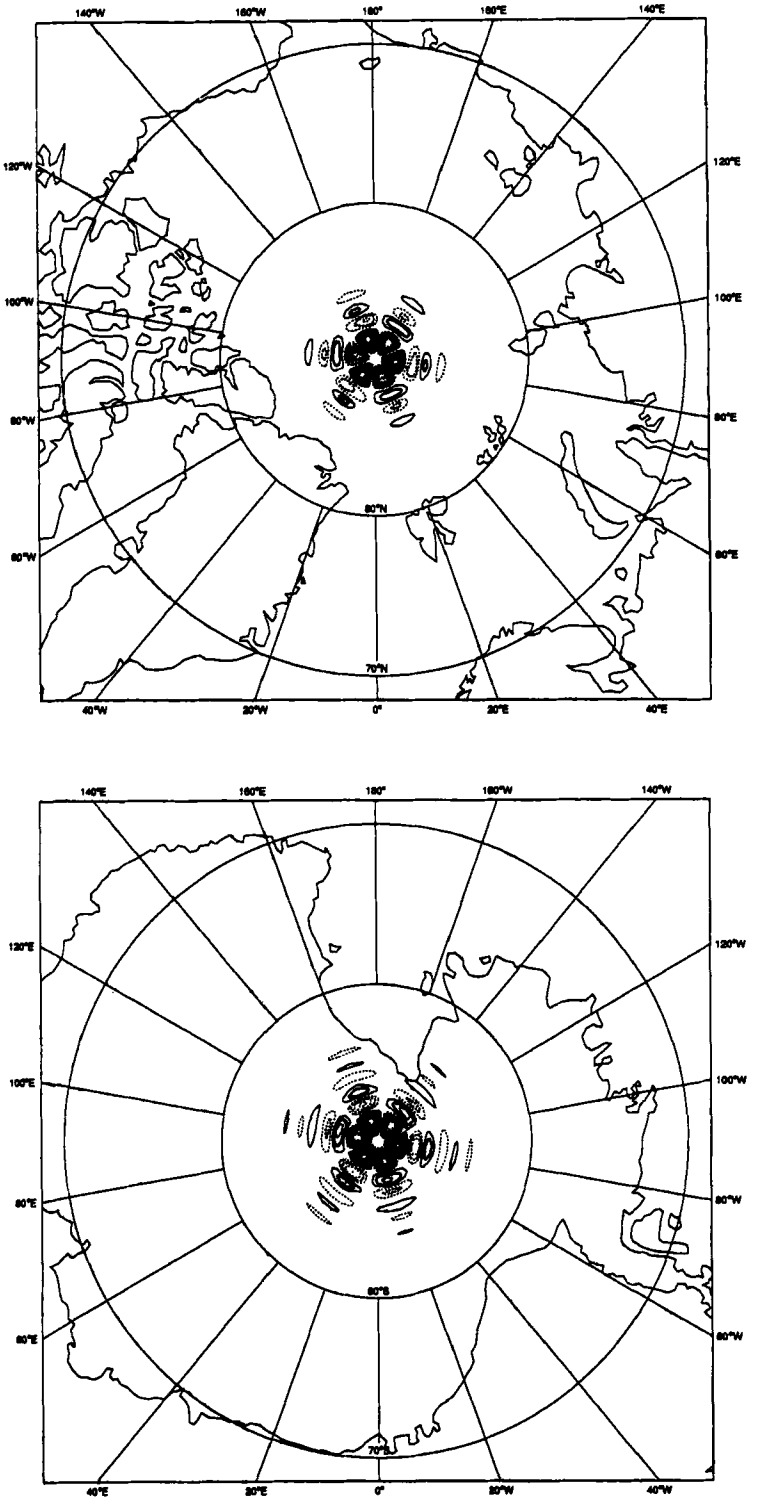

Figure 7. Impact on the vorticity field of going 300 times from spectral to grid point and back again. 6, 12 and 18 points are used on the first three latitude rows. Isoline: $2 \times 10^{-7} s^{-1}$. Top: northern pole area; bottom: southern pole area.

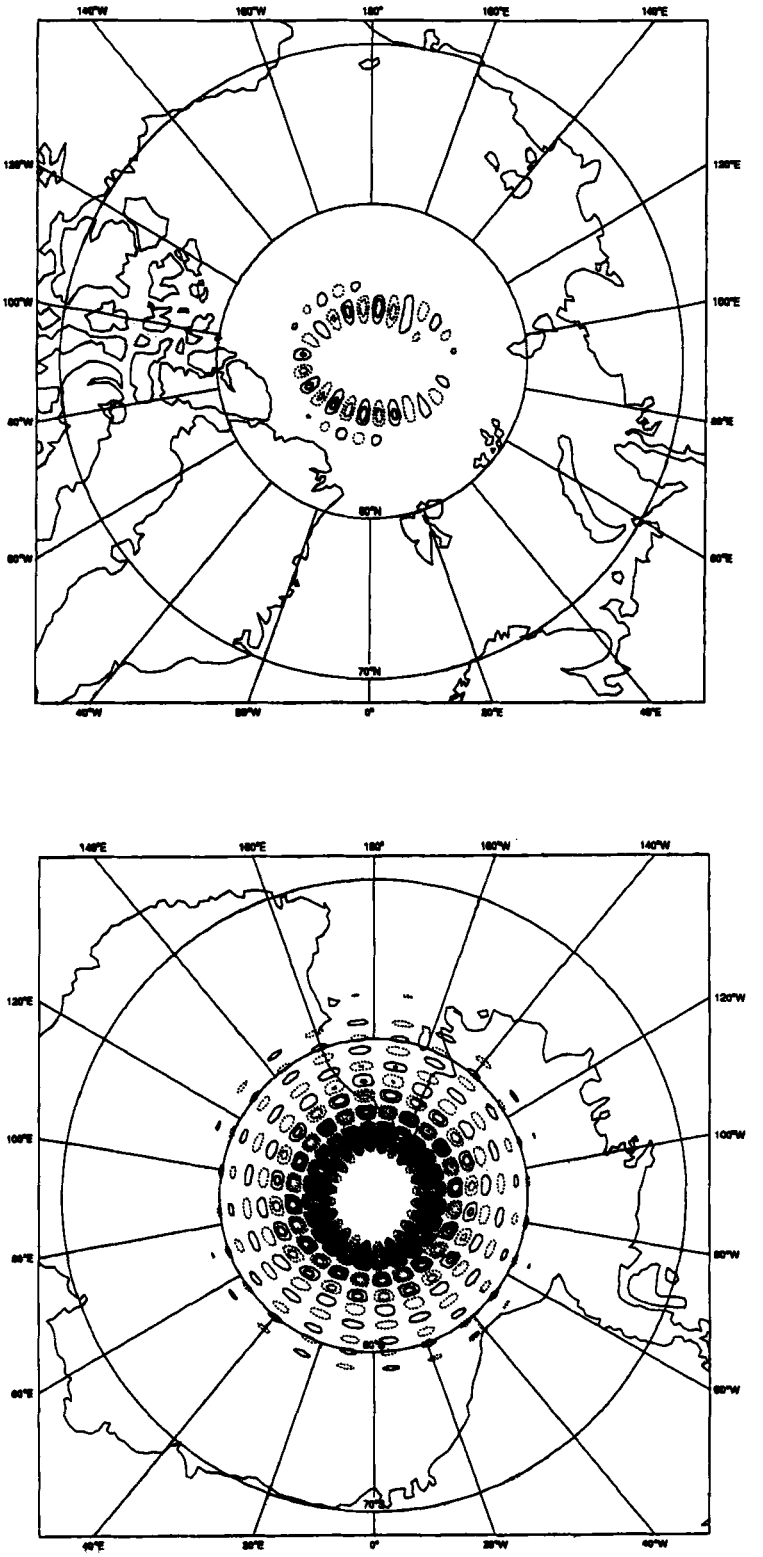

Figure 8. Same as Fig. 7 but with 12, 16 and 20 points. Isoline: $4 \times 10^{-9} s^{-1}$.

term, exacerbated in one case and not in the other. One should notice that, in a shallow-water model, the u–v and the vorticity–divergence formulation are algebraically equivalent, as Ritchie (1988) has shown. In a three-dimensional model, where higher-order terms are present, they are not equivalent, as was shown by Rochas and Courtier (1992).

The increase in the number of points close to the pole, which is necessary so as to have a 10^{-12} grid, is marginal. The increase in points for having aliasing smaller than 10^{-4} is significant at T106 (11%), but twice as small at T213. The corresponding increase for aliasing smaller than 10^{-2} at T213 is 3%.

ACKNOWLEDGEMENTS

We thank Adrian Simmons for his comments on the first version of the manuscript, and Ryad El Khatib (Météo-France) for checking that the aliasing 10^{-4} is a good compromise—cost versus accuracy. The careful typing of the manuscript is due to Carole Edis.

APPENDIX 1

In a Galerkin method, one has to solve linear systems of the form

$$\mathbf{Mx} = \mathbf{y}$$

where $\mathbf{M}$ is the mass matrix. The mass-matrix elements are the inner product of two basic functions. When the basic functions are orthonormal, $\mathbf{M} = \mathbf{I}$ and solving the linear systems is trivial. Let us now assume that $\mathbf{M} = (\mathbf{I} + \varepsilon\mathbf{A}) + \mathrm{O}(\varepsilon^2)$ where $\mathbf{A}$ is of order unity. Then solving the linear system by putting $\mathbf{x} = \mathbf{y}$ introduces an error equal to $\varepsilon\mathbf{Ay}$. If we assume the values of $\mathbf{y}$ to be of order unity, then the error is of order $n\varepsilon$ where n is the order of the matrix $\mathbf{A}$ (and the size of the vectors $\mathbf{x}$ and $\mathbf{y}$). In order for the error $n\varepsilon$ to remain constant (and hopefully below some chosen threshold), ε has to decrease as n^{-1}.

APPENDIX 2

Asymptotic formulae for the associated Legendre functions where the order n and the co-latitude θ tend, respectively, toward infinity and zero, while $x = (2n + 1)\sin(\theta/2)$ and the zonal wavenumber m are kept constant

Modifying formulae 58 (p. 248, Robin 1958) so as to account for the normalization of the associated Legendre functions used in meteorology, and considering only integer values for n, we have

$$P_n^m(\cos\theta) = \left(\frac{2n+1}{2}\right)^m (2n+1)^{1/2}\left\{\frac{(n-m)!}{(n+m)!}\right\}^{1/2}\left\{J_m(x) + \mathrm{O}\left(\frac{1}{n^2}\right)\right\} \qquad \text{(A.2.1)}$$

where the co-latitude θ and the total wavenumber n tend together, respectively, to 0 and to $+\infty$, such that $x = (2n + 1)\sin(\theta/2)$ remains constant. In this appendix m is constant;

J_m is a Bessel function of the first kind. The following asymptotic properties hold:

$$\left(\frac{2n+1}{2}\right)^m = n^m\left(1+\frac{m}{2n}+\mathrm{O}(n^{-2})\right)$$

$$\left\{\frac{(n-m)!}{(n+m)!}\right\}^{1/2} = \{(n+m)(n+m-1)\ldots n\ldots(n-m+1)\}^{-1/2}$$

$$= n^{-m}\left\{1-\frac{m}{2n}+\mathrm{O}(n^{-2})\right\}.$$

We then have

$$P_n^m(\cos\theta) = (2n+1)^{1/2}\left\{J_m(x)+\mathrm{O}\left(\frac{1}{n^2}\right)\right\}. \tag{A.2.2}$$

Let us now consider θ_k, the k^{th} zero of the Legendre polynomial of degree N. An asymptotic formula which is used to initiate the Newton loop of the computation of Gaussian latitudes (Rochas and Courtier 1992; Abramowitz and Stegun 1964, formula 22.16.6) is

$$\theta_k = \frac{4k-1}{4N+2}\pi + \frac{1}{8N^2}\cot\frac{4k-1}{4N+2}\pi + \mathrm{O}(N^{-3}).$$

Consider the value of k fixed (x is to first order constant), then

$$\theta_k = \frac{4k-1}{4N}\pi\left\{1+\frac{2}{(4k-1)^2\pi^2}\right\} + \mathrm{O}(N^{-2}).$$

Put $N = \alpha n + \mathrm{O}(1)$, then

$$P_n^m(\cos\theta_k) = (2n)^{1/2}\{J_m(x_k)+\mathrm{O}(n^{-1})\}$$

with

$$x_k = \frac{4k-1}{4\alpha}\pi\left\{1+\frac{2}{(4k-1)^2\pi^2}\right\}.$$

Consider now an example which numerically validates the asymptotic formula. For the wavenumber 106 of the first latitude row of a T106 grid, we have $\alpha \approx 1.5$, $n = 106$ and $k = 1$. Then

$$P_{106}^m(\cos\theta_1) \approx 14.6 J_m(1.6).$$

From Abramowitz and Stegun (1964), Table 9.2, we find

$$J_8(1.6) = 3.8\times10^{-6} \qquad J_9(1.6) = 3.4\times10^{-7}$$

so

$$P_{106}^8(\cos\theta_1) \approx 5.6\times10^{-5} \qquad \mathrm{P}_{106}^9(\cos\theta_1) \approx 5.0\times10^{-6}.$$

This verifies the good accuracy of the asymptotic approximation since the values computed with double precision, using the stable Belousov formula (Rochas and Courtier 1992), lead to the result

$$P_{106}^8(\cos\theta_1) = 5.496\times10^{-5} \qquad \text{and } P_{106}^9(\cos\theta_1) = 4.891\times10^{-6}.$$

APPENDIX 3

Convergence of $P_n^m(\cos\theta)$ towards zero as $n \to \infty$ while n and m are linked by the relationship $m = n \sin\phi$

The proof resolves into three cases, namely

$$n - m = O(n), \quad n - m \ll n \quad \text{and } n = m.$$

We make use of Formula 78k p. 261 of Robin (1958) which describes the asymptotic behaviour of $P_n^m(\cos\theta)$ when n tends toward $+\infty$ together with m. Denoting by $\sin\phi$ the ratio m/n ($m = n\sin\phi$) and introducing the formula $M = n(\sin^2\phi - \sin^2\theta)^{\frac{1}{2}}$, we have

$$P_n^m(\cos\theta) \approx \left\{\frac{n!^2}{(n+m)!(n-m)!}\right\}^{1/2} \frac{1}{(\pi)^{1/2}} \frac{(n\cos\theta + M)^{n+1/2}(m\cos\theta - M)^m}{n^m(n-m)^m M^{1/2}\sin^m\theta} \qquad \left(\theta < \phi < \frac{\pi}{2}\right).$$

Using Stirling's formula $n! \approx (2\pi)^{\frac{1}{2}} e^{-n} n^{n+1/2}$, we have

$$\left\{\frac{n!^2}{(n+m)!(n-m)!}\right\}^{1/2} \approx \left\{\frac{(1-\sin\phi)^m}{\cos^{2n+1}\phi(1+\sin\phi)^m}\right\}^{1/2}.$$

Furthermore, the following equations apply:

$$(n\cos\theta + M)^{n+1/2} = n^{n+1/2}\{\cos\theta + (\sin^2\phi - \sin^2\theta)^{1/2}\}^{n+1/2} \qquad M^{1/2} = n^{1/2}(\sin^2\phi - \sin^2\theta)^{1/2}$$

$$(m\cos\theta - M)^m = n^m\{\sin\phi\cos\theta - (\sin^2\phi - \sin^2\theta)^{1/2}\}^n \qquad (n-m)^m = n^m(1-\sin\phi)^m$$

so

$$P_n^m(\cos\theta) \approx \frac{1}{\pi^{1/2}}\left\{\frac{\cos\theta + (\sin^2\phi - \sin^2\theta)^{1/2}}{\cos\phi(\sin^2\phi - \sin^2\theta)}\right\}^{1/2}\{f(\phi)\}^n = A(\phi)\{f(\phi)\}^n$$

with

$$f(\phi) = \frac{\cos\theta + (\sin^2\phi - \sin^2\theta)^{1/2}}{\cos\phi}\left\{\frac{\sin\phi\cos\theta - (\sin^2\phi - \sin^2\theta)^{1/2}}{\cos\phi\sin\theta}\right\}^{\sin\phi}.$$

We are reminded that θ (the latitude under consideration) is constant. ϕ is also constant and determines the ratio m/n as m and n tend toward infinity. It then remains to prove that $f(\phi) < 1$ for $\theta < \phi < \frac{1}{2}\pi$ so as to establish the convergence of $P_n^m(\cos\theta)$ towards zero. After a few manipulations and using the formulae

$$(\sin^2\phi - \sin^2\theta)^{1/2} = (\cos^2\theta - \cos^2\phi)^{1/2} = \{\sin(\theta+\phi)\sin(\phi-\theta)\}^{1/2},$$

we obtain

$$f(\phi) = \frac{\{(\cos\theta + \cos\phi)^{1/2} + (\cos\theta - \cos\phi)^{1/2}\}^2}{2\cos\phi}\left[\frac{2\sin\theta\cos\phi}{\{\sin^{\frac{1}{2}}(\theta+\phi) + (\sin^{\frac{1}{2}}(\phi-\theta)\}^2}\right]^{\sin\phi}$$

so we have $f(\phi) > 0$ and $f(\theta) = 1$. Let us show that f is a decreasing function of ϕ in the interval $[\theta, \frac{1}{2}\pi]$ or, equivalently, that $\log f$ is decreasing. Once this is established, we shall have proved that $f(\phi) < 1$.

$$\log f(\phi) = 2\log\{(\cos\theta + \cos\phi)^{1/2} + (\cos\theta - \cos\phi)^{1/2}\} - \log 2 - \log\cos\phi +$$
$$+ \sin\phi\log(2\sin\theta) + \sin\phi\log\cos\phi - 2\sin\phi\log\{\sin^{\frac{1}{2}}(\theta+\phi) + \sin^{\frac{1}{2}}(\phi-\theta)\}$$

and

$$\frac{d\log f(\phi)}{d\phi} = \frac{-\sin\phi(\cos\theta+\cos\phi)^{-1/2} + \sin\phi(\cos\theta-\cos\phi)^{-1/2}}{(\cos\theta+\cos\phi)^{1/2}+(\cos\theta-\cos\phi)^{1/2}}$$

$$+\frac{\sin\phi}{\cos\phi} + \cos\phi\log(2\sin\theta) +$$

$$+\cos\phi\log\cos\phi - \frac{\sin^2\phi}{\cos\phi} - 2\cos\phi\log\{(\sin^{\frac{1}{2}}(\theta+\phi)+\sin^{\frac{1}{2}}(\phi-\theta)\} -$$

$$-\sin\phi\frac{\cos(\theta+\phi)\sin^{-\frac{1}{2}}(\theta+\phi)+\cos(\phi-\theta)\sin^{-\frac{1}{2}}(\phi-\theta)}{\sin^{\frac{1}{2}}(\theta+\phi)+\sin^{\frac{1}{2}}(\phi-\theta)}$$

which can be transformed as

$$\frac{d\log f(\phi)}{d\phi} = \cos\phi\log\underbrace{\frac{2\sin\theta\cos\phi}{\{\sin^{\frac{1}{2}}(\theta+\phi)+\sin^{\frac{1}{2}}(\phi-\theta)\}^2}}_{A} +$$

$$+\frac{\sin\phi}{\sin^{\frac{1}{2}}(\theta+\phi)\sin^{\frac{1}{2}}(\theta-\phi)}\left\{\frac{-(\cos\theta-\cos\phi)^{1/2}+(\cos\phi+\cos\phi)^{1/2}}{(\cos\theta+\cos\phi)^{1/2}+(\cos\theta-\cos\phi)^{1/2}}+\right.$$

$$+\frac{1-\sin\phi}{\cos\phi}\{\sin(\theta+\phi)\sin(\phi-\theta)\}^{1/2}$$

$$\left.-\underbrace{\frac{\cos(\theta+\phi)\sin^{\frac{1}{2}}(\phi-\theta)+\cos(\phi-\theta)\sin^{\frac{1}{2}}(\theta+\phi)}{\sin^{\frac{1}{2}}(\theta+\phi)+\sin^{\frac{1}{2}}(\phi-\theta)}}_{B}\right\}.$$

Consider first $A(\phi)$. We have $A(\theta)=1$. A is a decreasing function of ϕ; the numerator and the denominator are both positive with the numerator decreasing and the denominator increasing with ϕ. Therefore $A(\phi)<1$ and $\cos\phi\log(A(\phi))\leqslant 0$.

B can be transformed further:

$$B(\phi) = \frac{\cos\theta-\{\sin(\theta+\phi)\sin(\phi-\theta)\}^{1/2}}{\cos\phi} + \frac{1-\sin\phi}{\cos\phi}\{\sin(\theta+\phi)\sin(\phi-\theta)\}^{1/2} +$$

$$+\frac{\sin\phi}{\cos\phi}\{\sin(\theta+\phi)\sin(\phi-\theta)\}^{1/2} - \frac{\sin\phi}{\sin\theta}$$

and

$$B(\phi) = \frac{\cos\theta}{\cos\phi} - \frac{\sin\phi}{\sin\theta} = \frac{\sin 2\theta-\sin 2\phi}{2\sin\theta\cos\phi}$$

B is therefore always negative.

f is a decreasing function of ϕ, so $f<1$ for $\phi>\theta$. $P_n^m(\cos\theta)$ converges towards zero exponentially.

In any interval $[\psi_1,\psi_2]$ such that $\theta<\psi_1<\psi_2<\frac{1}{2}\pi$, $A(\psi)$ is bounded and $(f(\phi))^n\leqslant(f(\psi_1))^n$ since f is a decreasing function. There is then uniform convergence toward zero for the first case, i.e. $n-m=O(n)$. It remains to extend the uniform convergence all the way to $\phi=\frac{1}{2}\pi$, i.e. to include the case $n-m\ll n$.

In the vicinity of $\frac{1}{2}\pi$, introducing $h=\frac{1}{2}\pi-\phi$, and considering the dominant term in h, we have the asymptotic formula (valid for $n-m$ large) leading to

$P_n^m(\cos\theta) \approx (2/\pi h)^{1/2}\sin^m\theta$. From this formula it is clear that uniform convergence can be extended further towards $\phi = \frac{1}{2}\pi$ than was stated in the previous paragraph by allowing $h \geq Kn^{-1/2}$ for some positive constant K. However the cases where $n = m$ and $n - m = O(1)$ still need to be considered separately. For $n = m$, a direct examination of $P_n^n(\cos\theta)$ shows that

$$P_n^n(\cos\theta) = \sin^n\theta\left\{\frac{(2n+1)!!}{2n!!}\right\}^{1/2}$$

$$\approx \sin^n\theta\left(\frac{2(2n+1)}{\pi}\right)^{1/4}.$$

For large n, the behaviour is dominated by $\sin^n\theta$ which ensures convergence towards zero.

The asymptotic behaviour for n large with $n - m \ll n$ is obtained by introducing $p = n - m$ into the formula (78 K, p. 261 of Robin 1958). First, using Stirling's formula, we have

$$\frac{(n!)^2}{(n+m)!(n-m)!} \approx \left\{\frac{2^p\pi^{1/2}(1-p/2n)^{p-1/2}}{p!}\right\}\frac{n^{p+1/2}}{2^{2n}}.$$

Next write

$$M = n\cos\theta\left[1 - \frac{p}{n\cos^2\theta} - \left(\frac{p}{n}\right)^2\frac{\sin^2\theta}{2\cos^3\theta} + O\{(p/n)^3\}\right]$$

so that

$$(n\cos\theta + M)^{n+1/2} = (2n\cos\theta)^{n+1/2}\left[1 - \frac{p}{2n\cos^2\theta} + O\{(p/n)^2\}\right]^{n+1/2}$$

$$\approx (2n\cos\theta)^{n+1/2}\exp\left(-\frac{p}{2\cos\theta}\right)$$

$$(n\cos\theta - M)^m = \left(\frac{p\sin^2\theta}{\cos\theta}\right)^m\left[1 + \frac{p}{2n\cos^2\theta} + O\{(p/n)^2\}\right]^m$$

$$\approx \left(\frac{p\sin^2\theta}{\cos\theta}\right)^m\exp\left(\frac{p}{2\cos^2\theta}\right)\left[1 + \frac{p}{2n\cos^2\theta} + O\{(p/n)^2\}\right]^{-p}.$$

Substituting these expressions and gathering terms gives

$$P_n^m(\cos\theta) \approx \left\{\frac{2}{\pi^{\frac{1}{2}}}\left(1 - \frac{p}{2n}\right)^{p-1/2}\frac{2^p n^{p+1/2}}{p!}\right\}^{1/2}(n\cos\theta)^p\left(1 + \frac{p}{2n\cos^2\theta}\right)^p\sin^m\theta.$$

This expression is clearly dominated by the term $\sin^m\theta$ for $p = O(1)$; If $p = O(n)$ this is no longer true since the terms n^p would then dominate. However it suffices that the term $\sin^m\theta$ still dominates for $p = O(n^{1/2})$ since the uniform convergence was seen, above, to extend that far. The uniform convergence thus holds for any interval $[\phi_1, \frac{1}{2}\pi]$, with $\phi_1 > \theta$.

Note that substituting $p = 0$ into this formula gives

$$P_n^m(\cos\theta) \approx \left(\frac{4n}{\pi}\right)^{1/4}\sin^n\theta$$

which agrees to a high degree with the direct formula obtained for $n = m$; however, it

was necessary to treat the case $n = m$ separately since the formula 78 k on p. 261 of Robin (1958) was established only for $m < n$.

REFERENCES

Abramowitz, M. and Stegun, I. 1964 *Handbook of mathematical functions*. Dover publications, Inc., New York

Bourke, W. 1972 An efficient one-level primitive-equation spectral model. *Mon. Weather Rev.*, **100**, 683–689

Dautray, R. and Lions, J.-L. 1985 *Analyse mathématique et calcul numérique pour les sciences et les techniques*. Tome 3. Masson, Paris

Hortal, M. 1991 'Formulation of the ECMWF model'. Pp. 261–280 in Vol. II, *Proc. 1991 ECMWF seminar on numerical methods for atmospheric models*. Available from ECMWF

Hortal, M. and Simmons, A. J. 1991 Use of reduced Gaussian grids in spectral models. *Mon. Weather Rev.*, **119**, 1057–1074

Jarraud, M. and Simmons, A. 1983 'The spectral technique'. Pp. 1–60 in Vol. II, *Proc. 1983 ECMWF seminar on numerical methods for weather prediction*. Available from ECMWF

Ritchie, H. 1988 Application of the semi-Lagrangian method to a spectral model of the shallow-water equations. *Mon. Weather Rev.*, **116**, 1587–1598

Robin, L. 1958 *Fonctions sphériques de Legendre et fonctions sphéroïdales*. Tome II. Gauthier-Villars, ed., Paris

Rochas, M. J. and Courtier, P. 1992 'La méthode spectrale en météorologie'. Note de travail *Arpege*, No. 30. Available from Météo-France, Paris

Simmons, A. J. 1991 Development of a high resolution, semi-Lagrangian version of the ECMWF forecast model. Pp. 281–324 in Vol. II, *Proc. 1991 ECMWF seminar on numerical methods for atmospheric models*. Available from ECMWF